Modeling of the cracks with hydro-mechanical coupling in saturated porous environment

Summary:

One proposes a new element of joint allowing to model in 2D discontinuities with coupling-hydromechanics. This element is used to net a crack or a way of crack in a grid of classical elements THM voluminal in the case of a saturated porous material. It makes it possible to model the behavior of a water seal or a crack under pressure of fluid.

One presents here the equations constitutive of mechanics and hydraulics in the crack as well as the corresponding laws of behavior. The adopted discretization is also detailed and the vector forces intern and the tangent operator introduced into the operator STAT_NON_LINE.

Contents

Contents

1 Introduction

One presents here a model of discontinuity in porous environment saturated with hydro-mechanical coupling which gives an account of the following coupled phenomena:

- the preferential flow of the liquid intersticiel in the joint, which depends on the opening of the crack,
- the exchanges of fluid enters it joint and the porous environment,
- deformation of the solid mass and the opening of crack under the action of the pressure of crack,
- propagation of the crack.

According to the law of behavior chosen, this model makes it possible to model the propagation of the crack or simply the behavior of a water seal already completely open. This element of joint rests on the formulation of the elements of joints already present in *Code_Aster* in classical mechanics [dj]. Hydraulic degrees of freedom are added in order to take into account the flow in the crack and the exchanges of fluid with the porous solid mass.
The propagation is represented by a model of cohesive zone and one uses the regularized cohesive laws of the mechanical elements of joints. In order to model the behavior of the water seals completion opened, one introduces the law of behavior of Bandis.
The way of crack is discretized by these elements of joint while the rest of the structure is with a grid by already existing elements THM voluminal in *Code_Aster* [dthm].

One describes here the conservation equations hydraulic and mechanical along discontinuity, the corresponding laws of behavior, as well as the digital integration of these equations.

This work lies within the scope of the GNR MoMas (program TB5, Excavation Ramming Zones).

2 Presentation of the problem

2.1 Assumptions

A porous environment, noted is considered Ω at the current moment and whose border is noted $\partial\Omega$. This volume is separate in two parts Ω^+ and Ω^- by an interface Γ . All sizes in Ω^+ (resp. Ω^-) of one + (reps are subscripted. of one -).

One under investigation limits porous environment saturated with two dimensions.

2.2 Notations

2.2.1 Mechanical magnitudes

The field of displacement in the solid mass and the discontinuity of displacement through the crack are noted respectively $\boldsymbol{u}=\begin{pmatrix} u_x \\ u_y \end{pmatrix}$ and $[\![\boldsymbol{u}]\!]=\begin{pmatrix} [\![u_x]\!] \\ [\![u_y]\!] \end{pmatrix}$.
The total constraint and the effective constraint are noted respectively σ and σ' in the solid mass and τ and τ' on the interface.

2.2.2 Hydraulic sizes

The pressure of pore of the fluid intersticiel is noted p^+ and p^- in the solid masses surrounding the crack. The pressure of fluid in the crack is noted p . The gradient of pressure in the solid masses is noted ∇p^+ or ∇p^- . The longitudinal gradient of the pressure of the crack is noted $\nabla_l p$ and is defined by

$$\nabla_l p = \nabla p - \frac{\partial p}{\partial n} \boldsymbol{n} \tag{2.2.1}$$

where $\boldsymbol{n}$ is the normal with the interface.

The mass contributions of fluid are noted m in the solid mass (unit: $M.L^{-3}$) . In the crack, they are noted w (unit: $M.L^{-2}$) and are integrated on the thickness ε crack:

Mass hydraulic flow in the solid mass is noted $\boldsymbol{M}$ (unit: $M.T^{-1}.L^{-2}$) . In the crack, the mass hydraulic flow is noted W (unit: $M.T^{-1}.L^{-1}$).

ε is the opening of the crack and is thus connected to the jump of normal displacement by

$$\varepsilon = \varepsilon_0 + [\![\boldsymbol{u}]\!].n \tag{2.2.2}$$

Where ε_0 is the initial thickness.

3 Continuous equations

3.1 Mechanics

3.1.1 Constitutive equations

The formulation of the models to cohesive zone and their digital integration are presented in the reference material [R7.02.11]. One makes a very short recall here of it.

The field of displacement is sought $\boldsymbol{u}$ with balance by minimization of energy

$$E(\boldsymbol{u}) = \int_{\Omega/\Gamma} \phi(\boldsymbol{\varepsilon}(\boldsymbol{u}))\, d\Omega - W^{\text{ext}}(\boldsymbol{u}) + \int_{\Gamma} \Psi([\![\boldsymbol{u}]\!])\, d\Gamma \tag{3.1.1}$$

where ϕ is the density of mechanical energy voluminal, W^{ext} is the work of the forces outsides and Ψ is the density of energy of surface.

The data of Ψ characterize the mechanical behavior of the interface. It is expressed by a cohesive law which connects the force of cohesion $\boldsymbol{\tau}$ who is exerted on the lips of the crack to the jump of displacement by:

$$\boldsymbol{\tau} = \frac{\partial \Psi}{\partial [\![\boldsymbol{u}]\!]} \tag{3.1.2}$$

In addition, one makes the assumption of the effective constraints. In the solid mass, the tensor forced total is broken up into:

$$\boldsymbol{\sigma} = \boldsymbol{\sigma}' + \sigma_p \boldsymbol{I} \tag{3.1.3}$$

where $\boldsymbol{\sigma}'$ indicate the effective constraint and σ_p the hydraulic constraint.

On discontinuity, the vector forced total is broken up into:

$$\boldsymbol{\tau} = \boldsymbol{\tau}' + \tau_p \boldsymbol{n} \tag{3.1.4}$$

where $\boldsymbol{\tau}'$ indicate the effective constraint.

3.1.2 Laws of behavior

3.1.2.1 Effective constraints

In the solid mass, one makes the assumption of the effective constraints of Biot for the saturated mediums, by introducing the hydraulic constraint σ_p function of the pressure p (in fact p^+ or p^- in the solid mass) such as:

$$\sigma_p = -b\, p \tag{3.1.5}$$

where b is the coefficient of Biot of material.

On discontinuity, within the framework of a model of cohesive zone, one distinguishes three zones:

- an open zone where the total constraint on the lips is equal to $p\,\boldsymbol{n}$;
- a zone of transition enters the open medium and the healthy medium. In this zone, one observes the appearance of microfissuring and plasticity. One thus makes the plastic assumption of incompressibility of the matrix and it is the effective constraint of Terzaghi which controls the opening of the zone. The total constraint is written then

$$\boldsymbol{\tau} = \boldsymbol{\tau}' - p\,\boldsymbol{n} \tag{3.1.6}$$

- a healthy zone where there are adherence and not interpenetration of the lips. As long as the value of the constraint remains lower than the critical stress, the opening remains worthless.

One thus makes the assumption, in coherence with the behavior of these three zones, that

$$\tau_p = -p \tag{3.1.7}$$

3.1.2.2 Cohesive laws

The model presented here is compatible with the cohesive laws whose energy is regularized into zero:

- CZM_LIN_REG,
- CZM_EXP_REG.

These laws make it possible to take into account:

- Noninterpenetration of the lips of crack by penalization;
- Propagation of crack by a lenitive law;
- The irreversibility of cracking.

The parameters material of the interface are the critical stress with the rupture σ_c and the energy of rupture G_c . The digital parameters are the parameter of regularization of energy PENA_ADHERENCE and the parameter of penalization of the interpenetration PENA_CONTACT.

3.1.2.3 Law of Bandis

In this case, the model of joint does not take into account the propagation of crack. The joint separates two solid masses while being open all length and is simply equipped with a law which connects the opening to the effective constraint.

In the case of the empirical law of Bandis[bandis], the relation between the normal effective constraint τ'_n and the closing of normal crack $U=U_{\max}-\varepsilon$ (where U indicate $[\![\boldsymbol{u}]\!].\boldsymbol{n}$) is given by

$$d\tau'_n=-K_{\mathrm{ni}}\frac{dU}{\left(1-\frac{U}{U_{max}}\right)^{\gamma}} \tag{3.1.8}$$

where U_{max} is the asymptotic closing of the crack, K_{ni} the normal initial rigidity of discontinuity and γ an empirical coefficient which varies between 2 and 6 and which depends on the surface roughness of the joint. The law of behavior (3.1.8) is represented in figure 3.1.1.

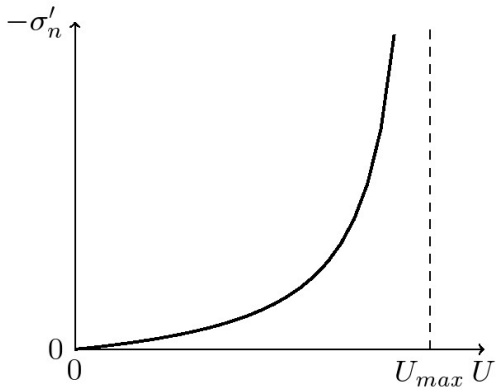

Illustration 3.1.1: Law of Goodman: curve constraint-closing

In the tangential direction, the behavior is supposed to be elastic.

$$\tau'_t=\tau_t=K_t[\![u_t]\!] \tag{3.1.9}$$

The keyword of *Code_Aster* correspondent with this law is JOINT_BANDIS. This keyword is to be informed in DEFI_MATERIAU like in the behavior (in RELATION_KIT).

3.2 Hydraulics

3.2.1 Constitutive equations

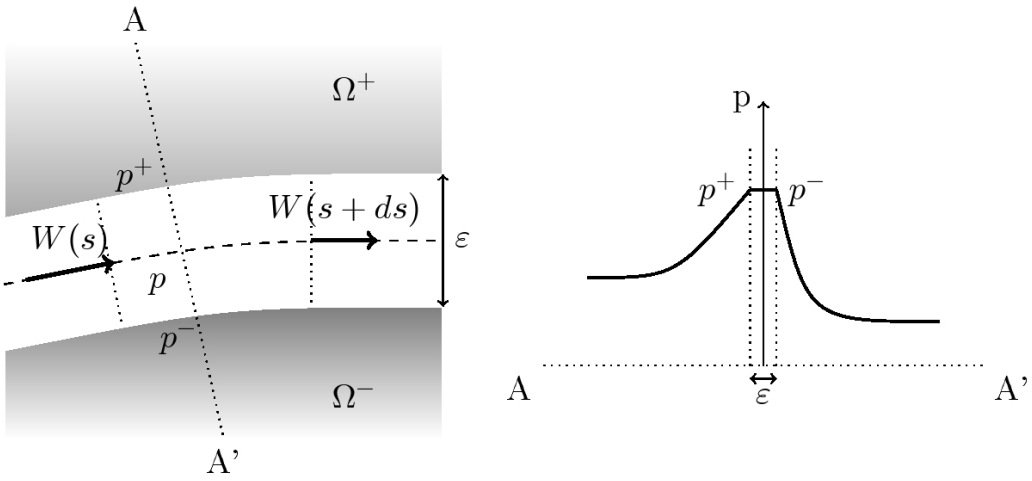

Illustration 3.2.1: conservation of the mass in the crack (on the left) and typical profile of pressure through the interface (on the right)

The conservation equation of the mass in the crack is written

$$\frac{\partial w}{\partial t}+\frac{\partial W}{\partial s}=0 \tag{3.2.1}$$

The thickness of crack being low, one considers that the field of pressure is continuous through the interface. In any point of the interface, one thus has

$$p_\Gamma^+ = p = p_\Gamma^- \tag{3.2.2}$$

On the other hand, discontinuities of flow are authorized through the interface (see figure 3.2.1 right-hand side)

3.2.2 Laws of behavior

The mass contributions of fluid in the open crack are written

$$w=\rho\,\varepsilon \tag{3.2.3}$$

Where ρ is the density of the fluid.
The evolution of the mass contributions is given by:

$$\frac{d\,w}{\rho}=\left(\frac{1}{N}+\frac{\varepsilon}{K_f}\right)d\,p+d\,\varepsilon \tag{3.2.4}$$

where K_f is the module of compressibility of the fluid and N the module of Biot of the cohesive zone.

It is considered that the flow in the crack is darcéen. Mass flow can thus be written

$$W=-\varepsilon\,\rho\,\lambda_H\left(\frac{\partial p}{\partial s}-\rho\,g\,\frac{\partial z}{\partial s}\right) \tag{3.2.5}$$

where λ_H is the hydraulic conductivity of the crack and Z indicates the coordinate along the vertical axis. It is given by

$$\lambda_H = \frac{K(\varepsilon)}{\mu(T)} \tag{3.2.6}$$

The relation between the flow and the gradient of pressure is given by the cubic law[cubiq]. Voluminal flow through the crack is written then

$$\frac{W}{\rho} = -\frac{\varepsilon^3}{12\mu}\left(\frac{\partial p}{\partial s} - \rho g \frac{\partial z}{\partial s}\right) \tag{3.2.7}$$

and the intrinsic permeability K according to the opening

$$K(\varepsilon) = \frac{\varepsilon^2}{12} \tag{3.2.8}$$

One notes T transmissivity of the crack, defined by

$$T = \varepsilon \lambda_H \rho = \frac{\rho \varepsilon^3}{12\mu} \tag{3.2.9}$$

This law is found analytically by the law of One tenth of a poise when one studies a laminar flow between two smooth plates separated by a distance ε small in front of other dimensions. Its validity was also put in obviousness on cracks in the rocks for a broad range of parameters[cubiq].

When the walls of crack are impermeable, one can model the solid mass with finite elements mechanical classics. In this case, the equation of flow becomes singular in the part of closed and not damaged crack. A parameter of regularization is thus introduced `OUV_FICT` who allows to have a fictitious flow in the part of closed crack. On the closed elements, one takes ε equal to `OUV_FICT`.

4 Variational formulation

4.1 Mechanics

One notes U_{ad} the whole of the acceptable fields of displacements, i.e. elements of $\left(H^1(\Omega)\right)^d$ checking the boundary conditions in displacement on the part of $\partial\Omega$ supporting such conditions.

Conditions of optimality for energy (3.1.1) give the following variational formulation:

$$\begin{cases} \boldsymbol{\sigma} = \boldsymbol{\sigma}' + \sigma_p \boldsymbol{I} \\ \boldsymbol{\tau} = \boldsymbol{\tau}' - p\,\boldsymbol{n} \\ \int_{\Omega\setminus\Gamma} \boldsymbol{\sigma} : \boldsymbol{\epsilon}(\hat{\boldsymbol{u}})\, d\Omega + \int_{\Gamma} \boldsymbol{\tau} . [\![\hat{\boldsymbol{u}}]\!]\, d\Gamma = W_{ext}(\hat{\boldsymbol{u}}) \qquad \forall \hat{\boldsymbol{u}} \in U_{ad} \end{cases} \tag{4.1.1}$$

4.2 Hydraulics

One notes P^+_{ad} (resp. P^-_{ad}) the whole of the acceptable fields of pressure on Ω^+ (resp. Ω^-), i.e. elements of $H^1(\Omega^+)$ (resp. $H^1(\Omega^-)$) checking the boundary conditions in pressure on $\partial\Omega^+_P$, the part of $\partial\Omega^+$ supporting boundary conditions in pressure, (resp. $\partial\Omega^-_P$). And one notes P_{ad} the whole of the acceptable fields of pressure on Γ, i.e. elements of $H^1(\Gamma)$ checking the boundary conditions in pressure on $\partial\Gamma_P$.

$$-\int_{\Omega^+}\frac{\partial m}{\partial t}\hat{p}^+ d\Omega+\int_{\Omega^+}\boldsymbol{M}.\nabla\hat{p}^+ d\Omega=\int_{\partial\Omega^+_F}\boldsymbol{F}.\boldsymbol{n}\,\hat{p}^+ d\Gamma+\int_\Gamma q^+\hat{p}^+ d\Gamma \quad \forall\hat{p}^+\in P^+_{ad} \tag{4.2.1}$$

$$-\int_{\Omega^-}\frac{\partial m}{\partial t}\hat{p}^- d\Omega+\int_{\Omega^-}\boldsymbol{M}.\nabla\hat{p}^- d\Omega=\int_{\partial\Omega^-_F}\boldsymbol{F}.\boldsymbol{n}\,\hat{p}^- d\Gamma+\int_\Gamma q^-\hat{p}^- d\Gamma \quad \forall\hat{p}^-\in P^-_{ad} \tag{4.2.2}$$

$$-\int_\Gamma\frac{\partial w}{\partial t}\hat{p}\,d\Gamma+\int_\Gamma W\nabla_l\hat{p}\,d\Gamma+\int_\Gamma\left(q^++q^-\right)\hat{p}\,d\Gamma=\int_{\partial\Gamma_F}\boldsymbol{F}.\boldsymbol{n}\,\hat{p}\,ds \quad \forall\hat{p}\in P_{ad} \tag{4.2.3}$$

$$\int_\Gamma\left(p^+-p\right)\hat{q}^+ d\Gamma=0 \quad \forall\hat{q}^+\in H^{-1}(\Gamma) \tag{4.2.4}$$

$$\int_\Gamma\left(p^--p\right)\hat{q}^- d\Gamma=0 \quad \forall\hat{q}^-\in H^{-1}(\Gamma) \tag{4.2.5}$$

4.3 Temporal discretization

One adopts a discretization in implicit time. Subscripted notations by n are the subscripted quantities at the beginning of step of time and those by $n+1$ are the quantities at the end of the step of time.

The step of time is noted $\Delta t=t_{n+1}-t_n$.

Thereafter, in the absence of precision, the nonsubscripted notations will indicate the sizes at the end of the step of time.

5 Construction of an element of joint

The trajectory of crack Γ is a priori defined, one can thus discretize it by elements of joint. Under-fields Ω^+ and Ω^-, located on both sides of Γ, are discretized by classical elements THM voluminal[dthm] so that their NœUDS with the interface coincide.

5.1 Degrees of interpolation of the degrees of freedom

The element of joint with hydro-mechanical coupling takes again the mechanical formulation of the classical elements of joint (but while passing from a linear element to a quadratic element) and interacts with close elements THM. The degrees of interpolation of degrees of freedom is thus chooses in coherence with these close elements.

In order to be compatible with elements THM of the solid mass:

- displacements are interpolated quadratically ($P2$ - continuous)

- the pressures are interpolated linearly ($P1$ - continuous).

A degree of freedom which does not preexist in any of the two preceding elements appears in the formulation. It is the hydraulic multiplier of Lagrange (variables q^+ and q^- in the variational equations 4.2.1 with 4.2.5). The degree of interpolation of these hydraulic multipliers of Lagrange must be chooses so as to observe a discrete condition LBB. They are thus taken constant by element.

5.2 Description of the element

The built element is worthless thickness and one nets the whole of the way of crack with this element. The lower and higher edges are connected to the rest of the structure. The flow of the fluid along the crack is written along the medium plan of the element (in gray on the figure 5.2.1).

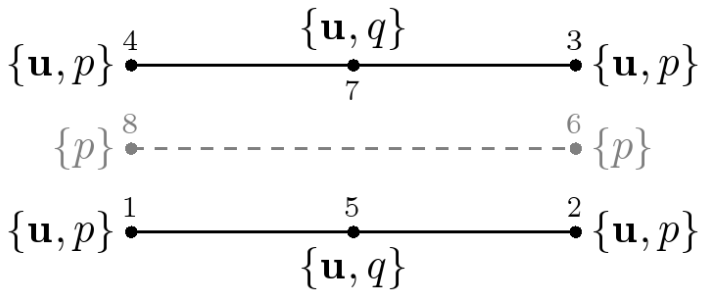

Illustration 5.2.1: "Burst" sight of the element of joint with hydro-mechanical coupling and without propagation

6 Algorithm of resolution

The variational problem (4.1.1-4.2.5) can be written in the form:

$$\boldsymbol{F}(\boldsymbol{U})=\boldsymbol{L}^{int}(\boldsymbol{U})-\boldsymbol{L}^{meca}=0 \tag{6.1}$$

where $\boldsymbol{U}$ indicate generalized displacements.

The associated tangent operator is noted $D\boldsymbol{F}=\frac{\partial \boldsymbol{F}}{\partial \boldsymbol{U}}$.

6.1 Generalized constraints and deformations

One notes $\boldsymbol{U}^{el}$ the vector of the nodal unknown factors on the element el, $\boldsymbol{E}_{pi}^{el}$ the vector of the deformations generalized at the point of integration pi element el, $\boldsymbol{\Sigma}_{pi}^{el}$ the vector of the generalized constraints

$$\boldsymbol{\Sigma}_{pi}^{el}=\begin{Bmatrix}\boldsymbol{\tau}'\\ -p\\ w\\ W\\ q^{+}\\ q^{-}\\ p^{+}-p\\ p^{-}-p\end{Bmatrix}^{el} \tag{6.1.1}$$

$$\boldsymbol{E}_{pi}^{el}=\begin{Bmatrix}[\![\boldsymbol{u}]\!]\\ p\\ \nabla p\\ p^{+}\\ p^{-}\\ q^{+}\\ q^{-}\end{Bmatrix}^{el} \tag{6.1.2}$$

The generalized deformations are obtained by the relation

$$\boldsymbol{E}_{pi}^{el}=\boldsymbol{Q}_{pi}^{el}.\boldsymbol{U}^{el} \tag{6.1.3}$$

where $\boldsymbol{Q}_{pi}^{el}$ is the matrix of passage of the nodal degrees of freedom to the deformations generalized at the point of integration pi. One calculates it starting from the functions of form and the orientation of the element. Indeed, mechanical displacements of each Nœud are defined in the total reference mark. In order to extract from them the components normal and tangential with the element from joint, a matrix of rotation is applied Θ_{pi}^{el} with the vectors nodal displacements.

6.2 Integration

To integrate on the element the terms of the vector, one chooses a method of selective integration. This one makes it possible to avoid the digital oscillations for the problems where the structure is subjected to a shock and where the mechanical phenomena prevail [select]. This method consists in integrating into the tops of the element the terms utilizing a derivative compared to time and integrating into the points of Gauss the permanent terms.

The vector forces intern is written

$$\boldsymbol{L}^{int}(\boldsymbol{U})=\sum_{el}\left(\sum_{g}\omega_{g}\boldsymbol{R}_{g}^{el}(\boldsymbol{U}^{el})+\sum_{s}\omega_{s}\boldsymbol{R}_{s}^{el}(\boldsymbol{U}^{el})\right) \tag{6.2.1}$$

while noting $\boldsymbol{R}_{g}^{el}$ and $\boldsymbol{R}_{s}^{el}$ values respectively at the point of Gauss g and at the top s nodal forces and ω_{g} and ω_{s} weights of integration respectively of g and s.

The tangent operator is written

$$D\boldsymbol{F}(\boldsymbol{U})=\sum_{el}\left(\sum_{g}\omega_{g}D\boldsymbol{F}_{g}^{el}(\boldsymbol{U})+\sum_{s}\omega_{s}D\boldsymbol{F}_{s}^{el}(\boldsymbol{U})\right) \quad (6.2.2)$$

while noting $D\boldsymbol{F}_{g}^{el}$ and $D\boldsymbol{F}_{s}^{el}$ values respectively at the point of Gauss g and at the top s of the tangent operator.

The tangent operator and the nodal forces are thus calculated differently at the points of Gauss and the tops. On the other hand, all the components of the generalized constraints and all the internal variables are calculated at the same time at the points of Gauss and the points of integration.

6.3 Vector internal forces: options RAPH_MECA and FULL_MECA

The following decomposition is adopted

$$\hat{\boldsymbol{E}}_{pi}^{el\,T}.\bar{\boldsymbol{\Sigma}}_{pi}^{el}=\bar{\boldsymbol{\Sigma}}_{\boldsymbol{u}}[\![\hat{\boldsymbol{u}}_{g}]\!]+\bar{\Sigma}_{p}\hat{p}+\bar{\Sigma}_{\nabla p}\nabla\hat{p}+\bar{\Sigma}_{p^{+}}\hat{p}^{+}+\bar{\Sigma}_{p^{-}}\hat{p}^{-}+\bar{\Sigma}_{q^{+}}\hat{q}^{+}+\bar{\Sigma}_{q^{-}}\hat{q}^{-} \quad (6.3.1)$$

where $\hat{\boldsymbol{E}}_{pi}^{el}=\left([\![\hat{\boldsymbol{u}}_{g}]\!],\hat{p},\nabla\hat{p},\hat{p}^{+},\hat{p}^{-},\hat{q}^{+},\hat{q}^{-}\right)$ is a virtual generalized deformation calculated starting from a vector virtual generalized displacement.

Starting from the discrete variational formulations and by distributing the stationary terms at the points of Gauss and the non stationary terms at the tops of the element, one obtains:

- at the points of Gauss

$$\begin{aligned}
\bar{\boldsymbol{\Sigma}}_{\boldsymbol{u}}^{el} &= \tau'-p_{g}\boldsymbol{n}\\
\bar{\Sigma}_{p}^{el} &= \Delta t\,(q_{g}^{+}+q_{g}^{-})\\
\bar{\Sigma}_{\nabla p}^{el} &= \Delta t\,W\\
\bar{\Sigma}_{p^{+}}^{el} &= -\Delta t\,q^{+}\\
\bar{\Sigma}_{p^{-}}^{el} &= -\Delta t\,q^{-}\\
\bar{\Sigma}_{q^{+}}^{el} &= p^{+}-p\\
\bar{\Sigma}_{q^{-}}^{el} &= p^{-}-p
\end{aligned} \quad (6.3.2)$$

- at the tops

$$\begin{aligned}
\bar{\boldsymbol{\Sigma}}_{\boldsymbol{u}}^{el} &= \boldsymbol{0}\\
\bar{\Sigma}_{p}^{el} &= w_{n}-w_{n+1}\\
\bar{\Sigma}_{\nabla p}^{el} &= 0\\
\bar{\Sigma}_{p^{+}}^{el} &= 0\\
\bar{\Sigma}_{p^{-}}^{el} &= 0\\
\bar{\Sigma}_{q^{+}}^{el} &= 0\\
\bar{\Sigma}_{q^{-}}^{el} &= 0
\end{aligned} \quad (6.3.3)$$

One has in addition:

$$\hat{\boldsymbol{U}}^{elT}.\boldsymbol{R}_{pi}^{el}=\hat{\boldsymbol{E}}_{pi}^{elT}.\bar{\boldsymbol{\Sigma}}_{pi}^{el} \tag{6.3.4}$$

what gives

$$\boldsymbol{R}_{pi}^{el}=\boldsymbol{Q}_{pi}^{elT}.\bar{\boldsymbol{\Sigma}}_{pi}^{el} \tag{6.3.5}$$

6.4 Tangent operator: options FULL_MECA and RIGI_MECA_TANG

The tangent operator at the point of Gauss g is given by:

$$\frac{\partial \boldsymbol{\Sigma}_g^{el}}{\partial \boldsymbol{E}_g^{el}}=\begin{bmatrix} \frac{\partial \tau_n'}{\partial [\![u_n]\!]} & \frac{\partial \tau_n'}{\partial [\![u_t]\!]} & -1 & 0 & 0 & 0 & 0 & 0 \\ \frac{\partial \tau_t}{\partial [\![u_n]\!]} & \frac{\partial \tau_t}{\partial [\![u_t]\!]} & 0 & 0 & 0 & 0 & 0 & 0 \\ 0 & 0 & 0 & 0 & 0 & 0 & \Delta t & \Delta t \\ \Delta t \frac{\partial W}{\partial u_n} & 0 & \Delta t \frac{\partial W}{\partial p} & -\Delta t\, T & 0 & 0 & 0 & 0 \\ 0 & 0 & 0 & 0 & 0 & 0 & -\Delta t & 0 \\ 0 & 0 & 0 & 0 & 0 & 0 & 0 & -\Delta t \\ 0 & 0 & -1 & 0 & 1 & 0 & 0 & 0 \\ 0 & 0 & -1 & 0 & 0 & 1 & 0 & 0 \end{bmatrix} \tag{6.4.1}$$

The tangent operator at the top s is given by:

$$\frac{\partial \boldsymbol{\Sigma}_s^{el}}{\partial \boldsymbol{E}_s^{el}}=\begin{bmatrix} 0 & 0 & 0 & 0 & 0 & 0 & 0 & 0 \\ 0 & 0 & 0 & 0 & 0 & 0 & 0 & 0 \\ -\frac{\partial w}{\partial [\![u_n]\!]} & 0 & -\frac{\partial w}{\partial p} & 0 & 0 & 0 & 0 & 0 \\ 0 & 0 & 0 & 0 & 0 & 0 & 0 & 0 \\ 0 & 0 & 0 & 0 & 0 & 0 & 0 & 0 \\ 0 & 0 & 0 & 0 & 0 & 0 & 0 & 0 \\ 0 & 0 & 0 & 0 & 0 & 0 & 0 & 0 \\ 0 & 0 & 0 & 0 & 0 & 0 & 0 & 0 \end{bmatrix} \tag{6.4.2}$$

The tangent operator at the point of integration pi is finally given by:

$$D\boldsymbol{F}_{pi}^{el}=\boldsymbol{Q}_{pi}^{elT}.\frac{\partial\boldsymbol{\Sigma}_{pi}^{el}}{\partial\boldsymbol{E}_{pi}^{el}}.\boldsymbol{Q}_{pi}^{el} \tag{6.4.3}$$

6.5 Vector nodal forces: option FORC_NODA

The option FORC_NODA is used by STAT_NON_LINE at the time of the phase of prediction.

At the point of integration pi, the vector nodal forces at time $n+1$ is defined by:

$$\boldsymbol{F}_{pi,n+1}^{el}=\boldsymbol{Q}_{pi}^{elT}.\bar{\boldsymbol{S}}_{pi}^{el} \tag{6.5.1}$$

where $\bar{\boldsymbol{S}}_{pi}^{el}$ is null at the tops and is given to the points of Gauss by:

$$\begin{aligned}
\bar{\boldsymbol{S}}_{\boldsymbol{u},n+1}^{el} &= \boldsymbol{\tau}_{g,n}-p_{g,n}\boldsymbol{n}\\
\bar{S}_{p,n+1}^{el} &= \Delta t\,(q_{g,n}^{+}+q_{g,n}^{-})\\
\bar{S}_{\nabla p,n+1}^{el} &= \Delta t\,W_{g,n}\\
\bar{S}_{p^{+},n+1}^{el} &= -\Delta t\,q_{g,n}^{+}\\
\bar{S}_{p^{-},n+1}^{el} &= -\Delta t\,q_{g,n}^{-}\\
\bar{S}_{q^{+},n+1}^{el} &= p_{g,n}^{+}-p_{g,n}\\
\bar{S}_{q^{-},n+1}^{el} &= p_{g,n}^{-}-p_{g,n}
\end{aligned} \tag{6.5.2}$$

6.6 Internal variables

As for the models of classical THM, the variables of 1 with $NVIM$ ($NVIM$ depending on the mechanical law of behavior used) relate to the law of mechanics used. The following internal variables are:

- V_{NVIM+1} : $\rho-\rho_0$, variation of the density,
- V_{NVIM+2} : ε , opening of the crack.
-

7 Validation

The following table recapitulates the cases tests of validation of the models presented in this note.

Title	Name of the test	Documentation	Model	Law
Axisymmetric modeling of a joint with hydraulic coupling.	wtna111	V7.33.11	AXIS_JHMS	JOINT_BANDIS
Negative mascon of a tank	wtnp125	V7.32.125	PLAN_JHMS	JOINT_BANDIS
Gas injection in a fractured porous environment	wtnp126	V7.32.126	PLAN_JHMS	JOINT_BANDIS
Tests of splitting per corner of the concrete under pressure of fluid	wtnp128	V7.32.128	PLAN_JHMS	JOINT_BANDIS CZM_LIN_REG CZM_EXP_REG

8 Bibliography

Contents

[dj] LAVERNE, J., “Éléments finis de joint en 2D et en 3D“, Manuel de référence de Code_Aster, [R3.06.09]
[dthm] CHAVANT C., “Modélisations THHM. Généralités et algorithmes.“, Manuel de référence du Code_Aster, [R7.01.10-A]
[bandis] BANDIS, S., LUMSDEN, A.C, BARTON, N. : “Fundamentals of rock joints deformation“, 1983, Int. Jour. Of Rock Mechanics and mining Science and Geomech. Abstr., 20(6), 249-68
[cubiq] WHITERSPOON, P.A., WANG, J.S.Y. WIWAI, K., GALE, J.E. : “Validity of cubic law for fluid flow in a deformable rock fracture“, 1980, Water Resour. Res., 16, 1016
[select] FERNANDES, R., CHAVANT, C., DU SUAUG, G., “Définition d'une modélisation à intégration sélective pour les couplages Thermo-Hydro-Mécaniques“, Note EDF R&D, [HT-66/05/012/A]

9 Description of the versions of the document

Version Aster	Author (S) or contributor (S), organization	Description of the modifications
10/02/10	B. Carrier	Initial text